Molecular Catalysis 589 (2026) 115593

Contents lists available at ScienceDirect

Molecular Catalysis

journal homepage: www.journals.elsevier.com/molecular-catalysis

The role of phenylalanines in the access channel of surface displayed unspecific peroxygenase from *Agrocybe aegerita*

Niklas Teetz, Sonja Schönrock, Dirk Holtmann *

Process Engineering in Life Sciences 2 – Electro Biotechnology, Karlsruher Institute of Technology, 76131 Karlsruhe, Germany

ARTICLE INFO

Keywords:
Unspecific peroxygenase
Oxyfunctionalization
Surface display
Substrate affinity
Enzyme catalysis

ABSTRACT

Unspecific peroxygenases are an emerging class of oxyfunctionalization enzymes with a broad substrate spectrum. The structure of their access channel, that allows substrates to enter the catalytic heme center, depends on the enzyme family. Short UPOs access channel is typically lined with aliphatic amino acids like leucine and isoleucine while long UPOs access channel is mostly lined with aromatic phenylalanines. The type of amino acids in the access channel aligns with the preferred substrate class for each enzyme family. In this study we exchanged each of the seven phenylalanines in the access channel of the best researched enzyme in this class, the unspecific peroxygenase from *Agrocybe aegerita*, with aliphatic amino acids and investigated how the substrate preference of the enzyme variants compares to the wildtype enzyme. For 15 enzyme variants resulting from substitutions of three phenylalanines in close proximity to the heme center, we conducted docking studies. The results supported our hypothesis, that the substrate preference would shift towards aliphatic substrates when phenylalanines are exchanged with aliphatic amino acids. Additionally, we constructed 35 mutant strains of the production host *Komagataella phaffii* for the expression and surface display of enzyme variants for all phenylalanines in the enzymeś access channel. Characterization of these enzyme variants revealed that substrate preference changed opposite to the hypothesis and docking results, decreasing activity for aliphatic substrates and increasing activity for aromatic ones. We concluded that steric conditions in the active site are more important to the enzymeś substrate preference then the nature of the amino acids and identified the most important residues for different substrates.

1. Introduction

Unspecific peroxygenases (UPOs, EC 1.11.2.1) are heme-thiolate enzymes of fungal origin. They catalyze a number of oxyfunctionalization reactions, like hydroxylations, epoxidations or oxygenations [1,2] on a variety of substrate classes (pharmaceuticals [3,4] as well as bulk chemicals in the substance classes of linear [5] and cyclic alkanes [6,7], fatty acids [8,9], alkylbenzenes [10,11], benzene derivates [12,13] and more [1,2]). Their reaction- and substrate scope is similar to that of P450 monooxygenases but, instead of nicotinamide cofactors and oxygen, UPOs require only hydrogen peroxide as oxidizing agent and oxygen donor. Mechanistically, the hydroxylation reactions catalyzed by UPOs follow the peroxide shunt pathway of P450 monooxygenases [14,15].

The class of UPOs can be divided into the two families of short UPOs (family I) and long UPOs (family II) [16,17]. Besides their difference in size (29 - 32 kDa for short UPOs and around 44 kDa for long UPOs) short UPOs typically build dimers through intermolecular disulphide bridges while long UPOs are monomeric with intramolecular disulphide bridges. Furthermore, the access channel to the heme bearing active site of short UPOs is wider and shorter than that of long UPOs. The access channels of short UPOs feature predominantly aliphatic amino acids (mostly leucine and isoleucine), while the access channels of long UPOs are clad with aromatic amino acids (7 Phe in the case of AaeUPO, the model enzyme for long UPOs, See Fig. 1) [2]. The difference in amino acids seems to correlate to the preferred substrates of each family. While short UPOs tend to prefer large aliphatic substrates like steroids, the preference for long UPOs generally is linear aromatic substrates like polycyclic aromatic hydrocarbons e.g. pyrenes [2,18–22]. The bulky phenylalanines of long UPOs and the resulting narrow access channel mostly prevent the access and catalysis of bulkier substrates. In the microbial enzyme alkane monooxygenase (AlkB), alkane hydroxylation is catalyzed and the access channel to the active site (in this case non-heme; two iron ions, coordinated by histidines) is very narrow and lined with aliphatic

* Corresponding author.
E-mail address: dirk.holtmann@kit.edu (D. Holtmann).

https://doi.org/10.1016/j.mcat.2025.115593
Received 16 September 2025; Received in revised form 5 November 2025; Accepted 6 November 2025
Available online 11 November 2025

amino acids (mostly Leu and Ile, like in short UPOs). In this enzyme, substitution of the aromatic tryptophan W62, positioned in the upper access channel and therefore interacting with longer aliphatic substrates, for a valine shifted the activity towards longer aliphatic substrates [23]. This supports the correlation between the chemical nature of amino acids in the access channel and the enzymes substrate preference.

In a recombinant variant of *Aae*UPO, PaDa-I [24], the substitution of the amino acid A77 against a leucine in the near vicinity of the heme centre (so called Fett mutant) improved regioselectivity in fatty acid and linear alkane hydroxylation and limited overoxidation compared to the "wildtype" PaDa-I [9]. Very recently, Schmitz and co-workers substituted aliphatic amino acids in the access channel of the short UPO from *Aspergillus brasiliensis* (*Abr*UPO) with aromatic amino acids to mimic the active site of *Aae*UPO PaDa-I and investigated the change in substrate preference. They identified several amino acid positions that affect the selectivity aromatic versus alkyl chain hydroxylations and showed, that mimicking the active site of *Aae*UPO PaDa-I shifts the chemoselectivity of *Abr*UPO towards that of *Aae*UPO PaDa-I [25]. Similarly, Knorrscheidt and co-workers showed, that introducing phenylalanines in positions of aliphatic amino acids in the short UPO of *Myceliophthora thermophila* (*Mth*UPO) improves the conversion, K_m and k_{cat} of the enzyme towards the aromatic substrate 5-nitro-1,3-benzodioxole (NBD) and were able to direct hydroxylation of naphthalene derivates, depending on the distinct mutations in the active site [26].

Rotilio and coworkers demonstrated that the structure of *Hypoxylon sp.* EC38 UPO (*Hsp*UPO), the only known momomeric short UPO, is very similar to that of *Aae*UPO, despite there only being a 30 % sequence identity [27]. In a superposition of both structures, they depicted what amino acids in the access channel of *Hsp*UPO correspond to which amino acids in the access channel of *Aae*UPO. In position of the phenylalanines F76, F188, F191 and F199 in the *Aae*UPO access channel, *Hsp*UPO features an aliphatic amino acid (3 leucines and 1 alanine, respectively).

The engineering of the substrate preference of UPOs is generally of industrial interest and has been the object of several studies. Some of those covered the hydroxylation of aliphatic or aromatic substrates specifically, as described above. However, the role of the phenylalanines in the access channel of *Aae*UPO has not yet been investigated thoroughly.

In this study, we exchanged the phenylalanines in the access channel of *Aae*UPO_PaDa-I with the aliphatic amino acids alanine, glycine, isoleucine, leucine and valine and investigated, how this effects substrate affinities, activity and selectivity of the enzyme. These five aliphatic amino acids differ significantly in size and polarity. While glycine features the smallest possible amino acid rest (an H-atom) and is considered a polar amino acid, the other four amino acids are unipolar and feature alkyl rests of various size, either with 1 C-atom (alanine), 3 C-atoms (valine) or 4 C-atoms (leucine and isoleucine). The access channel of short UPOs are predominantly lines with the larger, more apolar aliphatic amino acids.

We exchanged the three phenylalanines involved in substrate positioning during catalysis *in silico* and conducted docking studies with the substrates NBD, cyclohexane, ethylbenzene, and hexane and compared the calculated affinity constants and predicted distances between heme and substrate for each of these enzyme variants to the ones of the wildtype *Aae*UPO PaDa-I and *Hsp*UPO. The four phenylalanines in the upper access channel are not involved directly during catalysis and were therefore disregarded for the docking studies. Furthermore, we constructed yeast strains for the surface display of all 35 enzyme variants (7 phenylalanines substituted by 5 aliphatic amino acids each), screened them for 2,2′-azino-bis(3-ethylbenzothiazoline-6-sulfonic acid) (ABTS) activity and investigated the six most active variants for ABTS, NBD, cyclohexane, ethylbenzene and hexane activity, stereoselectivity and reaction selectivity. The substrates were chosen as representatives for different substrate groups (ABTS: peroxidase activity; NBD: aromatic substrates; cyclohexane: cyclic aliphatic substrates; ethylbenzene: aromatic substrates that get hydroxylated on aliphatic rest; hexane: aliphatic substrates) and because they have been shown to be oxyfunctionalized by *Aae*UPO PaDa-I.

The surface display of UPOs was recently shown to be an effective immobilization method, that simultaneously simplifies downstream processing [28,29]. In this study we utilize the easy purification and concentration workflow enabled by this immobilization strategy to screen immobilized enzyme variants. Because the immobilization of UPOs often leads to detrimental activity reduction [29,30], screening enzymes in the already immobilized state can reduce overall effort needed to find enzyme variants with high activity when immobilized.

2. Methods

2.1. Docking studies

For each substrate and enzyme variant combination, 10 runs of semi-flexible docking via AutoDock 4.2 (Scripps Reasearch Institute, La Jolla, CA, USA) were performed with a genetic algorithm. Substrates were docked against the structure of *Aae*UPO PaDa-I (PDB entry: 5OXU) or variants of it, were phenylalanines were exchanged against aliphatic amino acids in PyMol, or the structure of *Hsp*UPO (PDB entry: 7O2G).

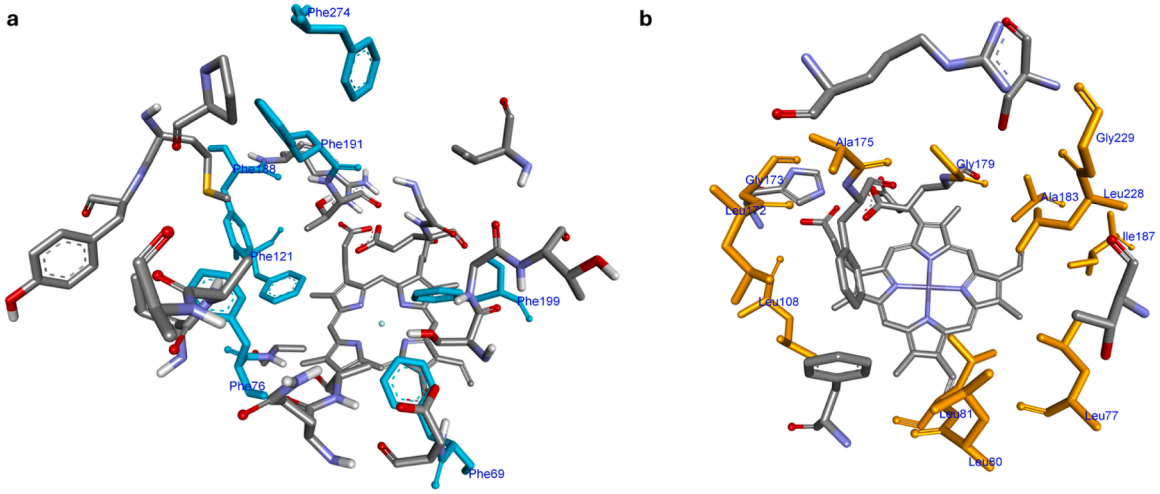

Fig. 1. Comparison of the amino acids lining the access channel of A: *Aae*UPO_PaDa-I (PDB entry: 5oxu); Phenylalanines are highlighted in blue and B: *Hsp*UPO (PDB entry: 7o2g); aliphatic amino acids are highlighted in orange.

Free water molecules in the structures were deleted beforehand, Kollmann charges were calculated, polar hydrogens added and histidine charges were calculated. Structures of substrates were downloaded from PubChem, their Gasteiger charges were calculated and torsion bonds defined. Each docking run had a starting population of 150 and maximally 2700 generations with 2.5 million evaluations were conducted while allowing a mutation rate of 0.02 and crossover rate of 0.8.

The results were clustered based on the calculated binding energy between substrate and enzyme in their final position and conformation. The best run from the cluster with the lowest mean binding energy was used as representative for this docking. The calculated k_a was taken from the results file created by AutoDock (listed as k_i). The value k_i is originally used to describe a concentration of an inhibitor molecule, that reduces the enzymes activity to 50 %. In this study, we did not dock inhibitor molecules but actual substrates. The k_i therefore describes the concentration of substrate at which half the enzyme is bound as enzyme-substrate complex. We used that concentration as k_a to define substrate affinity of the enzymes. The substrate-enzyme complex was exported as .pdb file and the distance between heme and substrate was determined in BIOVIA Discovery Studio (Dassault Systèmes, France).

2.2. Cloning

The plasmids coding for enzyme variants were produced by exchanging codons on the integration vector pPpB1_*Aae*UPO_PaDaI_SAG1 [28], isolated from a NEB 5-alpha *Escherichia coli* strain, by site specific mutagenesis using Q5® High-Fidelity DNA Polymerase (NEB, New England Biolabs, Ipswich, United States). 0.5 μg of the linear PCR products with exchanged codons were 5′ phosphorylated by T4-polynucleotide kinase (PNK; 0.5 μg linear DNA, 1 μL 10x ligase buffer (NEB), nuclease free water to 10 μL, 0.2 μL T4-PNK (10,000 U mL^{-1}; NEB) for 30 min at 37 °C. Subsequent inactivation of T4-PNK was performed at 65 °C for 20 min. After cooling on ice, the ends of the phosphorylated DNA were ligated by T4 ligase (NEB; 10.2 μL phorphorylation reaction, 2 μL ligase buffer (NEB), nuclease free water (NEB) to 20 μL, 1 μL T4-ligase (2000,000 U mL^{-1}, NEB)) for 2 h at RT. T4-ligase was then inactivated by incubation at 65 °C for 10 min. Subsequently, the template vector was digested via *Dpn*I digestion (20.2 μL ligation reaction, 2.5 μL rCutSmart buffer (NEB), 1 μL *Dpn*I (20,000 U mL^{-1}, NEB), nuclease free water to 25 μL) for 25 min at 37 °C. Plasmids were purified with the Monarch® Plasmid Miniprep Kit (NEB) following the manufacturer's instructions. The entire eluted, purified plasmids were used to transform competent *E. coli* NEB® 5-alpha cells following the manufacturer's instructions. The transformed cells were plated on (low salt) LB agar plates with 25 μg mL^{-1} zeocin and the plates were incubated at 37 °C for 16 – 24 h. Colonies were picked into 30 μL sterile water each and a colony PCR was performed using 1 μL of that cell suspension, confirming the presence of the *Aae*UPO_PaDa-I gene in the clone. For positive clones, the remaining 29 μL of cell suspension were used to inoculate 3 mL LB with 25 μg mL^{-1} zeocin and the cultures were incubated at 37 °C, 180 rpm, at a 45° angle in a cultivation tube for 16 h. Subsequently, a cryoculture of the clone was created by mixing 0.5 mL of the culture and 0.5 mL 50 % glycerine and stored at −80 °C. Furthermore, plasmid preparation was performed, using the Monarch® Plasmid Miniprep Kit (NEB) following the manufacturer's instructions. The correct sequence of the modified *Aae*UPO PaDa-I gene on the isolated plasmid was then confirmed by Sanger sequencing (Economy Run, Microsynth AG, Balgach, Switzerland).

2.3. Screening

Plasmids with the confirmed sequence were linearized by *Pme*I digestion (1 μg plasmid DNA, 5 μL rCutSmart buffer (NEB), 1 μL *Pme*I (10000 U mL^{-1}, NEB), nuclease free water to 50 μL) at 37 °C for 15 min and purified using the NucleoSpin® Gel & PCR Clean-up Kit (Macherey Nagel GmbH & Co. KG, Dueren, Germany) before transformation into *Komagataella phaffii*. Electrocompetent cells of *K. phaffii* X33 were transformed with the linearized plasmids and plated on YPDS agar + 100 μg mL^{-1} zeocin. Plates were incubated at 30 °C for 3 days and afterwards, colonies were picked into 900 μL BMGY medium (100 mM potassium phosphate buffer pH 6, 10 g L^{-1} yeast extract, 20 g L^{-1} peptone, 10 g L^{-1} glycerol, 400 μg L^{-1} biotin, 3.2 mM $MgSO_4$, 1.7 g L^{-1} yeast nitrogen base without amino acids, 10 g L^{-1} $(NH_4)_2SO_4$) with 100 μg mL^{-1} zeocin in wells of a 96-deep-well-plate (30 – 50 clones per strain). The plates were sealed with a Breathe-Easier membrane (Diversified Biotech Inc., Dedham, MA, USA) and incubated at 30 °C, 900 rpm on a ThermoMixer® C (Eppendorf SE, Hamburg, Germany) for 48 h. Afterwards, 10 μL per well were used to inoculate the wells of a second plate with 900 μL YPD medium (20 g L^{-1} peptone, 20 g L^{-1} dextrose, 10 g L^{-1} yeast extract) with 100 μg mL^{-1} zeocin and the YPD plate was incubated under identical conditions. In the BMGY plate, 100 μL of BMMY medium (100 mM potassium phosphate buffer pH 6, 10 g L^{-1} yeast extract, 20 g L^{-1} peptone, 5 g L^{-1} methanol, 400 μg L^{-1} biotin, 3.2 mM $MgSO_4$, 1.7 g L^{-1} yeast nitrogen base without amino acids, 10 g L^{-1} $(NH_4)_2SO_4$) were added per well and the plate was incubated further. After 24 h and 48 h each, 10 μL pure methanol was added per well. After a total of 120 h of incubation, enzyme activity was determined.

2.4. Determination of enzyme activities

2.4.1. ABTS assay

To determine the enzymes peroxidase activity, oxidation of 2,2′-azino-bis(3-ethylbenzothiazoline-6-sulfonic acid) (ABTS) was routinely measured. For the assay, 840 μL McIlvane buffer (pH = 4.5) and 100 μL 3 mM ABTS were incubated in a photometer's cuvette holder at 30 °C for at least 10 min. 10 μL of cell culture was added and the reaction was started by addition of 50 μL of 40 mM H_2O_2. Absorbance at 420 nm was measured and enzyme activity was calculated via the Beer-Lambert law based on the extinction coefficient of ABTS $\varepsilon_{420} = 36000\ M^{-1}\ cm^{-1}$.

2.4.2. NBD assay

To screen for peroxygenase activity, the model substrate 5-nitro-1,3-benzodioxole (NBD) was used. O-dealkylation of this substrate produces 4-nitrocatechol, which can be monitored at 425 nm. For the assay, 865 μL 100 mM potassium phosphate buffer and 100 μL 5 mM NBD (dissolved in acetonitrile) are heated to 30 °C, 10 μL sample are added and the reaction is started with addition of 25 μL of 40 mM H_2O_2. Absorbance at 425 nm was measured and activity calculated based on the extinction coefficient of 4-nitrocatechol $\varepsilon_{425} = 9700\ M^{-1}\ cm^{-1}$.

2.4.3. Ethyl benzene, cyclohexane, hexane

Catalysis of ethyl benzene, cyclohexane and hexane hydroxylation was conducted in 1.5 mL glass vials (HPLC sample vials), closed with two butyl septa, fixed by a screw cap. Assay conditions were optimized for each substrate with surface displayed *Aae*UPO PaDa-I to allow for high sensitivity of the assays. For ethyl benzene and cyclohexane hydroxylation, 525 μL of cell suspension (OD = 500) with surface displayed enzyme in 100 mM potassium phosphate buffer and 175 μL acetone with 1 M substrate were added into the vials. Vials were inverted on a rotator (intelli-mixer, neoLab Migge GmBH, Heidelberg, Germany) at 60 rpm on program F (rocking motion instead of full rotation) to allow for connection of a syringe pump (KD LEGATO® 111, kdScientific, Holliston, MA, USA; equipped with 3D-printed extensions to accommodate for 10 × 1 mL syringes) for hydrogen peroxide addition. Catalysis was conducted for 6 h with a feed rate of 5.8333 μL h^{-1} of 100 mM H_2O_2. Subsequently, the reaction mixture was transferred to a 1.5 mL reaction tube, 300 μL of ethyl acetate with 1 mM 1- octanol (internal standard) was added, the mixture rigorously shaken on a vortex mixer, left to rest for at least 2 min and centrifuged. The ethyl acetate phase was then subjected to GC analysis (Agilent DB-WAX 30 m, 0.25 mm, 0.25 μm; 3 μL injection, 1:10 split ratio; 40 °C for 5 min, 25 °C min^{-1} to 250 °C, 250 °C for 5 min; detection via flame ionization

detector). The activity was calculated from the increase of product over time.

For hexane hydroxylation, 350 μL cell suspension (OD =500) with surface displayed enzyme and 350 μL acetone with different hexane concentrations (10 mM to 4 M in acetone ≙ 5 mM to 2 M in the assay) were added into vials and rotated like described above. Catalysis was conducted for 8, 16 and 24 h with a feed of 2.9167 μL h^{-1} 100 mM H_2O_2. Extraction was done with 300 μL cyclohexane and the procedure and GC analysis were done as described above. A linear regression was performed over the three product amounts at 8, 16 and 24 h and activity was calculated from the slope of this regression.

3. Results

3.1. Docking studies

To understand substrate binding and its involved amino acids in the enzymes active site and access channel, we conducted *in silico* docking studies with *Aae*UPO (PDB entry 5oxu) and a variety of substrates with different chemical properties. We docked the linear alkane hexane, the cyclic alkane cyclohexane, the aromatic benzene derivate and common UPO substrate ethylbenzene and the surrogate NBD to the enzymes access channel and active site region. We were able to identify three phenylalanines (F69, F121, F199) in the enzymes active site that coordinate the position of most substrates during catalysis and set them as our targets for *in silico* mutagenesis to predict substrate affinity for the enzyme variants via further docking studies. In addition, the access channel region of the enzyme features four more phenylalanines (F76, F188, F191, F274) that line its inside but are not directly involved in substrate positioning during catalysis. The effects of mutagenesis of these amino acids would not show in docking studies but their exchange to aliphatic amino acids could still improve the enzymes affinity towards aliphatic substrates. In literature, the nature of the access channel lining amino acids is correlated to the enzyme's substrate preference [18] but the causation has not yet been proven. Therefore, we changed the 3 active site phenylalanines with the 5 aliphatic amino acids glycine, alanine, leucine, isoleucine and valine *in silico* and repeated docking studies with hexane, cyclohexane, ethyl benzene and NBD to predict changes in substrate coordination during catalysis. For all performed docking combinations, the respective calculations resulted in only one cluster of productive docking poses (the few exceptions are pointed out below). For the predictions concerning the docking we determined the distance between the heme species in the catalytic centre of the enzyme and the substrate and compared the calculated substrate affinity constant (k_a) (Table 1 &2; Tab SI 1 & 2). We did not dock 2,2′-azino-bis (3-ethylbenzothiazoline-6-sulfonic acid) (ABTS) to the enzymes active site. Although ABTS is commonly used as screening substrate for UPOs, it was not included in the *in silico* investigation because the ABTS oxidation is not indicative of peroxygenase activity but rather of peroxidase activity.

To assess the predicted results, docking was also conducted with *Hsp*UPO (PDB entry: 7o2g), a member of the short UPO family which shares strong structural similarity with *Aae*UPO_PaDa-I [27]. Indeed, this methodology led to the prediction of some variants, with decreased affinity towards aromatic substrates (higher k_a) and improved affinity towards aliphatic substrates (lower k_a) while distances to the heme were practically identical.

For example, the aromatic surrogate substrate NBD is stabilized in the active site of *Aae*UPO PaDa-I through π-π interactions between the substrate's benzene ring and the phenylalanines F69 and F76 (Fig. 2a). These interactions lead to a high affinity (low k_a) of *Aae*UPO PaDa-I towards NBD (Table 1). If F69 is substituted with an aliphatic amino acid like leucine, NBD is positioned more upright within the active site, not only having no π-π interaction to the amino acid in position 69 but also losing the π-π interaction with F76 in favour of a π-sigma bond between T192 and NBD (Fig 2b). This leads to a much lower predicted affinity (higher k_a) of F69L towards NBD than for *Aae*UPO PaDa-I (Table 1).

Table 1
Overview over the affinity constants (k_a) and heme-ligand distances of wildtype *Aae*UPO PaDa-I, *Hsp*UPO and all access channel variants of *Aae*UPO PaDa-I for the substrate 5-nitro-1,3-benzodioxole (NBD). Results are ordered by increasing k_a and divided into the categories: *Aae*UPO-PaDa-I; *Hsp*UPO; enzyme variants with k_a <1000; 1000 < k_a < 2000; 2000 < k_a.

NBD	Calculated k_a [μM]	Distance heme – ligand [Å]
*Aae*UPO-PaDa-I	206	2.960
F121G	494	5.909
F121I	610	3.238
F121V	722	4.178
F199A	729	2.930
F199V	790	3.286
F121A	974	4.165
F121L	1010	4.235
F199G	1160	2.259
F69V	1350	2.975
*Hsp*UPO	1710	6.048
F199I	1770	3.316
F199L	1830	3.178
F69L	2020	3.097
F69G	2030	3.037
F69A	2050	3.034
F69I	2060	3.127

Conversely, the aliphatic substrate hexane is merely held in place by van der Waals and π-alkyl interactions between the phenylalanines and the substrate in *Aae*UPO PaDa-I, leading to a low substrate affinity (Fig. 2c). In F69L, the substitution of phenylalanine for the smaller leucine opens up a new pocket inside the active site, in which the hexane can find a position where it not only interacts with the L69, but also with three additional alanines A73, A74 and A77 (Fig 2d). This leads to an increase in substrate affinity as can be seen by a lower calculated k_a (Table 2).

Docking results for the substrates cyclohexane and ethylbenzene with wildtype *Aae*UPO PaDa-I, the 15 enzyme variants F69X, F121X and F199X and *Hsp*UPO are summarized in the supporting information (Fig SI 1 - 17; Tab. SI 1 & 2).

In general, any investigated amino acid exchange of phenylalanine to an aliphatic amino acid improved affinity towards the aliphatic hexane and decreased affinity towards the aromatic NBD. However, the predicted affinity strongly depends on which amino acid is substituted. Substitution of F69 leads to the strongest changes for affinity towards NBD, from a k_a of 206 μM (*Aae*UPO PaDa-I) to over 2000 μM for F69A, F69G, F69I and F69L. Distances from heme to the substrate remain in a similar range to the "wildtype" *Aae*UPO PaDa-I. F69V also shows an increase in k_a but only to 1350 μM. Substitutions of F121 lead to moderately increased k_a between 494 μM and 1010 μM. However, the distances between the heme and the ligand C-atom that gets hydroxylated are increased compared to the wildtype *Aae*UPO PaDa-I. Except for F121I, distances increased for >1 Å, which will likely result in unproductive enzymes for the catalysis with this substrate. For substitutions of F199, the results depend on the amino acid that F199 was substituted with, ranging to predicted k_a from 729 μM to 1830 μM for F199A and F199L, respectively. The docking of NBD with *Hsp*UPO predicted an affinity constant of 1710 μM, which is in the range of the F69 substitutions, F199I and F199L but the distance between NBD and the heme is over 6 Å, which would not result in a hydroxylation of the substrate.

The affinity of *Aae*UPO PaDa-I towards hexane was improved by every substitution of phenylalanines with aliphatic amino acids. The calculated affinity constant of *Aae*UPO PaDa-I was 9380 μM and between 2000 μM and 3000 μM for most variants. Exceptions are F69V and F199G (1460 μM and 1790 μM, respectively) and F199I (3500 μM). The distances of the heme of *Aae*UPO PaDa-I to the C1, C2 and C3 atoms of hexane are in line with the regio-selectivity of the enzyme, which preferably hydroxylated the C2 and C3 atom in wet-lab experiments [5].

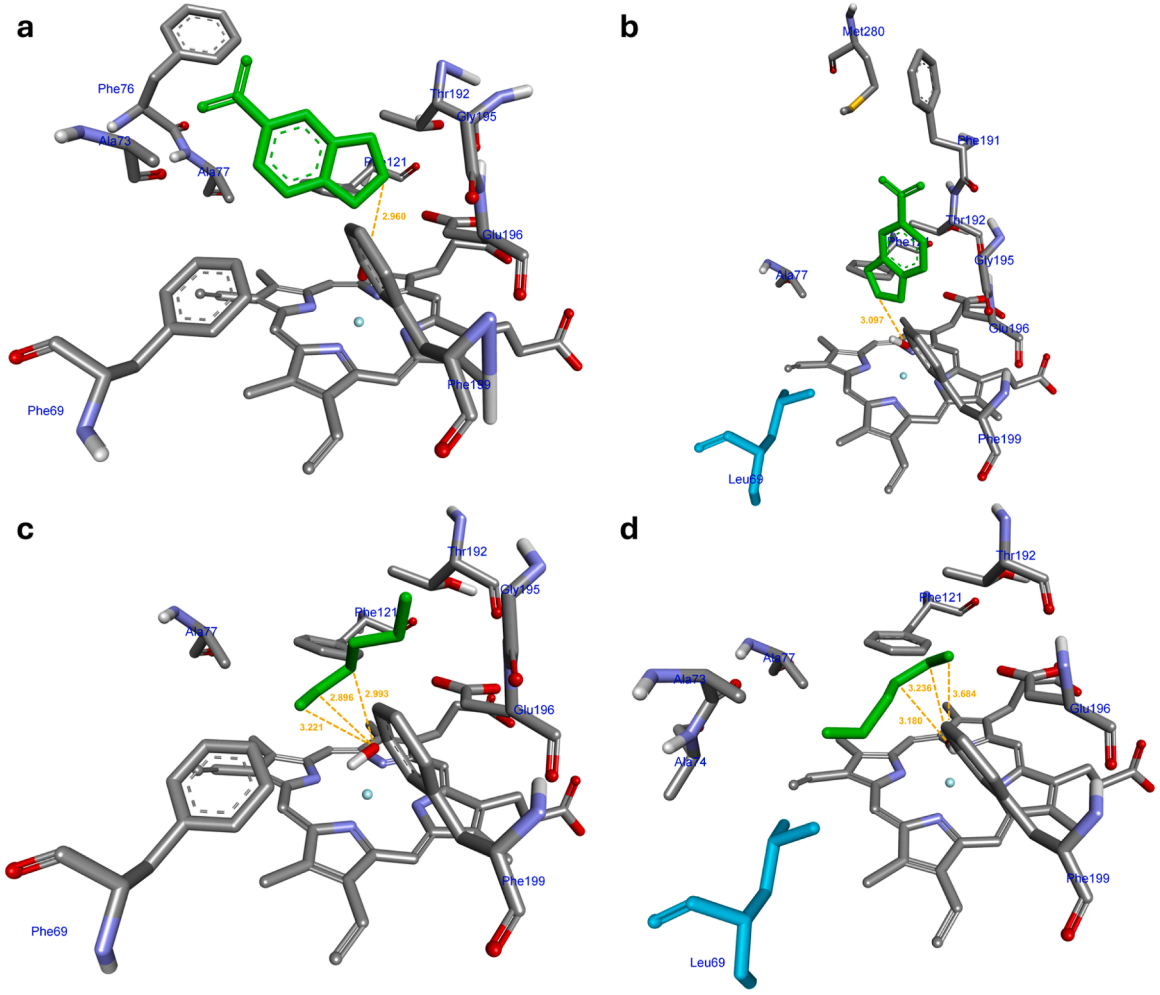

Fig. 2. Exemplary docking results of wildtype *Aae*UPO_PaDa-I and the variant F69L with the substrates NBD and hexane a: Docking of NBD and *Aae*UPO PaDa-I. b: Docking of the variant F69L with NBD. c: Docking of hexane and *Aae*UPO PaDa-I. d: Docking of the variant F69L with hexane. Substrates are highlighted in green, exchanged amino acids in light blue and distances are given in orange.

Table 2
Overview over the affinity constants (k_a) and heme-ligand distances (for the hexanes carbon atoms C1 – C3) of wildtype *Aae*UPO PaDa-I, *Hsp*UPO and all access channel variants of *Aae*UPO PaDa-I for the substrate hexane. Results are ordered by increasing k_a and divided into the categories: *Aae*UPO PaDa-I; *Hsp*UPO; enzyme variants with $k_a < 2000$; $2000 < k_a$.

Hexane	k_a [μM]	Distance heme C1 [Å]	Distance heme C2 [Å]	Distance heme C3 [Å]
F69V	1460	3.129	3.137	4.654
F199G	1790	3.558	3.148	4.128
F121I	2040	3.532	3.089	3.015
F69G	2120	3.787	4.968	4.930
F121V	2150	3.502	3.249	3.010
F199A	2180	3.002	3.532	3.212
F121A	2210	3.146	3.089	3.108
F121L	2300	3.584	4.121	3.636
F69A	2310	3.184	3.599	5.098
F199V	2420	2.949	3.386	3.063
F121G	2480	3.158	3.234	3.046
F69I	2600	3.568	3.134	3.649
F69L	2790	3.684	3.236	3.180
F199L	2940	3.342	3.310	2.921
F199I	3500	3.268	3.344	2.914
*Hsp*UPO	4280	2.860	3.014	3.664
*Aae*UPO PaDa-I	9380	3.221	2.896	2.993

Following this logic, we predicted different regioselectivities for many of the variants. We expected F69A, F199A and F199V to show preferred or exclusive terminal hydroxylation of hexane because of the larger distances between heme and C2 and C3 compared to C1. This would be in line with results from Olmedo and co-workers, that showed preferred terminal hydroxylation of alkanes by the short UPO from *Marasmius rotula* (*Mro*UPO) [31], which features predominantly aliphatic amino acids in its heme access channel [32]. Similarly, *Hsp*UPO, the short UPO we did docking studies with, also shows the lowest predicted distance from the heme to the C1 atom of hexane, indicating preferred terminal hydroxylation. For a concise overview about the hexane docking results, see Table 2.

For the cyclic alkane cyclohexane and ethylbenzene, that is an aromatic substrate but does not get hydroxylated on the benzene ring but on its aliphatic alkyl chain, the docking studies predicted varying results, depending on the substitution. For these substrates, changes in k_a are not as drastic as for NBD or hexane but the affinity for ethylbenzene does improve slightly to moderately for all amino acid substitutions investigated. The strongest improvement from the k_a of *Aae*UPO PaDa-I (957 μM) was calculated for variant F69G (362 μM) and the lightest improvement for F199I (930 μM). However, both of them and most of the substitutions of F69 and F199 lead to substrate-enzyme complexes where the distance between heme and substrate is likely too far for productive hydroxylation (Tab. SI 1). The most promising variants are F121A and F121G (k_a =489 μM for both, heme-substrate distances =

3.043 Å and 2.972 Å, respectively). Results for *Hsp*UPO are very similar to those of *Aae*UPO PaDa-I. For cyclohexane, some variants were predicted to have lower and some were predicted to have higher affinity, depending on the substitution (Tab. SI 2). Heme-substrate distances are in a productive range for all variants except F69A and F69G and k_a values for the other variants range from 921 μM (F199G) to 2280 (F69I), compared to *Aae*UPO PaDa-Is 1550 μM. *Hsp*UPO is predicted to have a k_a of 1470 μM.

3.2. Wet-lab experiments

To confirm our docking study results and test activity and enantioselectivity of the enzyme variants, we constructed 35 enzyme variants (7 phenylalanines, each mutated to 5 aliphatic amino acids) in the wet lab and expressed them as a yeast surface display. This allowed us to directly screen the variants in their immobilized state and furthermore simplified the purification out of the culture broth. After screening 30 – 50 clones per strain for the most active clone in 96-deep-well plates, we produced each strain in baffled shake flasks and measured peroxidase activity with ABTS and peroxygenase activity with NBD.

15 of the 35 variants produced at least one active clone in an ABTS screening (5 clones with mutations in the active site and 10 with mutations in the access channel) (Fig. 3). None of the substitutions at position F199 had any measured activity and substitutions at position F121 only had minimal activity. The only phenylalanine position in the active site that could be substituted while preserving a reasonable amount of activity was F69. Interestingly, the NBD activity of some variants was higher than that of the wildtype *Aae*UPO PaDa-I. This is also the case for F69L, although the docking studies predicted the opposite effect.

A hexane assay of the 15 variants revealed that, contrary to the *in silico* prediction, hexane activity was minimal or non-existent. However, we showed before, that activity per cell is influenced by cultivation parameters and that cultivation in a bioreactor leads to higher activity per cell than shake flask cultivations [33]. Because the *Aae*UPO PaDa-I control was produced in a bioreactor, we produced the 4 variants with highest hexane activity as well as F69L and F199L due to their interesting ABTS/NBD activity ratio in a larger quantity in a parallelized bioreactor (Sixfors®, Infors AG, Bottmingen, Switzerland).

The subsequent characterization revealed that hexane activity of all variants was indeed lower than in the wildtype enzyme. However, regioselectivity for F76L and F188G improved in comparison to *Aae*UPO PaDa-I (see Tab. SI 5). While the variants with substitutions in the upper access channel maintained some of their hexane activity (although barely measurable for F76G), the variants F69L and F199L, where phenylalanines in close vicinity to the heme centre were substituted, show no hexane activity at all. Ethylbenzene activity was also worse for all variants than for the wildtype. Within the variants, ABTS and ethylbenzene activities seem to be opposing. Stereoselectivity, for the variants with sufficient activity for measurement, did not improve (see Tab. SI 6). The variants F69L and F199L showed the highest occurrence of S-phenylethanol (30.8 % and 37.7 %, respectively, versus 0 % for *Aae*UPO PaDa-I). In continuity to the prediction of substrate affinity, the docking studies predicted the opposite effect, with *Aae*UPO PaDa-I presenting a substrate position that would result in S-phenylethanol (Fig. SI 1) and both these variants presenting a substrate position resulting in R-phenylethanol (Fig. SI 6 and 16). Noticeably, the occurrence of the overoxidation product acetophenone in reactions with ethylbenzene was strongly influenced by the introduced amino acid substitutions, although it is unlikely, that all of the observed effect can be attributed to the substitution alone (see Tab. SI 7 for details). However, 3 of the variants showed increased NBD activity over the wildtype and one of them (F76L) additionally had improved ABTS activity. Two variants (F69L and F199L) showed a drastically different preference between ABTS and NBD (higher NBD activity than ABTS). Activities can be viewed in Fig. 4. We judged the affinity towards aliphatic versus aromatic substrates by the proportion of the NBD and hexane activity. For F69L and F199L, that did not exhibit any hexane activity, this was not possible. All other variants show a drastically increased NBD activity/hexane activity ratio compared to *Aae*UPO PaDa-I (SI Tab. 3), indicating a change in substrate preference towards aromatic substrates which directly contradicts the authors original hypothesis.

3.3. Reactions with cyclohexane and production of 3-hydroxy-3-methyl-2-butanone

For a full characterization, we also tried to measure the cyclohexane activity of the wildtype and all enzyme variants. The wildtype *Aae*UPO PaDa-I did produce cyclohexanol as expected. Interestingly, none of the

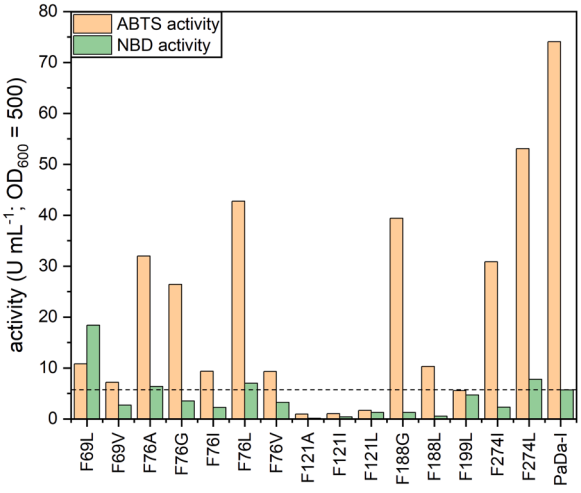

Fig. 3. Comparison of ABTS- and NBD-activities of yeast surface displayed enzyme variants with at least one active clone (most active clone is shown) in comparison to the wildtype enzyme *Aae*UPO PaDa-I. Assays were performed at 30 °C for 1 min and absorptions were measured every 0.1 s. Activities were calculated from the linear ($R^2 \geq 0.95$) adsorption increase at the start of the reaction. ABTS and NBD activities are normalized to U mL^{-1} and $OD_{600} = 500$. The NBD activity of *Aae*UPO PaDa-I is indicated with a dashed horizontal line.

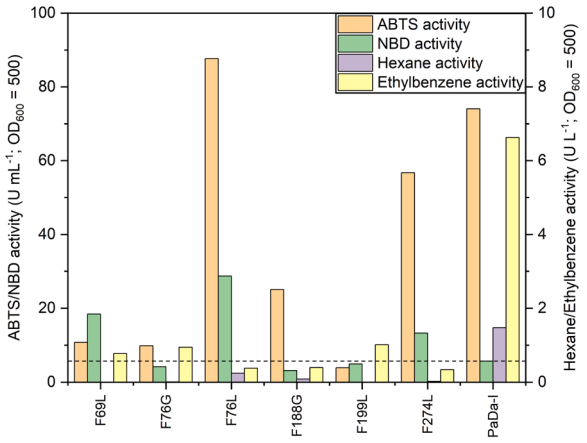

Fig. 4. Comparison of ABTS-, NBD-, hexane- and ethylbenzene activities for bioreactor-produced, surface displayed *Aae*UPO_PaDa-I and access channel variants. ABTS and NBD assays were performed at 30 °C for 1 min and absorptions were measured at 420 nm and 425 nm, respectively, every 0.1 s. Activities were calculated from the linear ($R^2 \geq 0.95$) adsorption increase at the start of the reaction. Hexane and ethylbenzene assays were performed at 20 °C for 24 h (hexane) or 6 h (ethylbenzene). Product amounts of the hexane and ethylbenzene catalysis were determined via GC analysis and activities calculated from the increase of product over time. Activities are normalized to U mL^{-1} (ABTS; NBD) or U L^{-1} (hexane; ethylbenzene) and $OD_{600} = 500$. The NBD activity of *Aae*UPO PaDa-I is indicated with a dashed horizontal line.

variants produced any cyclohexanol or cyclohexanone from cyclohexane. Instead, a different substance was produced, which was identified to be 3-hydroxy-3-methyl-2-butanone by first GC–MS analyses. The amount of product is different between enzyme variants based on the detected peak area and control runs with free *Aae*UPO PaDaI or *Hsp*UPO enzyme (no cells of *K. phaffii* present) or cells of *K. phaffii* (no UPO present)do not produce it. This indicates that the product is indeed a catalysis product of the enzyme variants. Furthermore, we discovered, that the enzyme variants produce 3-hydroxy-3-methyl-2-butanone even without the presence of cyclohexane, but the product amount is increased in the presence of cyclohexane. Elucidation of the production mechanism of 3-hydroxy-3-methyl-2-butanone is highly interesting but not within the scope of this current study. Results of GC–MS analysis and control experiments as well as a discussion of the production mechanism can be found in the supporting information (SI chapter 1.3, Fig SI 19, Tab. SI 4).

4. Discussion

In this study, we investigated how the nature of the amino acids in the access channel of *Aae*UPO PaDa-I, the model enzyme for long UPOs, influences the enzymes substrate affinities. We hypothesized, that exchanging the abundant, aromatic phenylalanines against aliphatic amino acids would shift the enzymes preference for aromatic substrates towards aliphatic substrates.

4.1. The working hypothesis was confirmed by docking studies

Our initial docking studies agreed with the hypothesis to a large degree. Every amino acid exchange led to a higher calculated affinity towards the aliphatic hexane and a decreased affinity towards the aromatic NBD. However, results for cyclohexane and ethylbenzene docking were not as conclusive. Ethylbenzene has an aromatic ring but is hydroxylated at its aliphatic ethyl rest. A logical continuation of our hypothesis would assume the biggest improvement in affinity for variants, where one of the three phenylalanines closest to the heme centre is exchanged with an aliphatic one to maintain aromatic affinity in the upper access channel but improve substrate orientation with the ethyl rest facing the heme. Docking studies were only conducted for the heme centre phenylalanine variants, so we were not able to test this *in silico* but every docking we performed predicted an increase in affinity, supporting this assumption. However, most variants are calculated to have their energetically most favourable position higher up in the access channel, in an unproductive distance to the heme. For cyclohexane, we expected similar results to the hexane docking because cyclohexane does not provide π-electrons for π-π interactions with the phenylalanines. Docking results however predicted, that affinity would be strongly dependent on the specific amino acid substitution, likely because of their differences in size and polarity.

4.2. The wet lab results mostly contradict the original hypothesis

Contrary to the docking results, the results from the characterization of our wet lab produced enzyme variants do not align with the original hypothesis. None of the variants with substitutions in the active site were able to hydroxylate hexane, although all of them showed increased affinity in the dockings. Conversely, NBD activity was predicted to be worse in all variants by the docking but was only moderately decreased in some variants and increased in others. For all bioreactor produced enzyme variants with both NBD and hexane activity, the ratio of these activities is indicating a higher preference for aromatic than for aliphatic substrates when compared to *Aae*UPO PaDa-I. These results were unexpected and falsify the hypothesis that prompted this study, at least for the investigated single substitution enzyme variants. The mismatch between the *in silico* docking studies and wet lab results can at least partially be attributed to the limitations of the used docking software for the simulation of enzyme-substrate dynamics, especially for metalloenzymes. Firstly, the software does not simulate the actual catalysis but rather predicts the energetically most likely position of the substrate in the framework of a rigid enzyme, which does not exactly represent the reality. Secondly, the iron atom in the centre of the heme in the active site of the enzyme is bound not only to the porphyrin molecule but also to a distal cysteine residue and to a water/hydrogen peroxide molecule. The software however only allows for a maximum of 4 bonds per atom (the bonds with the porphyrin), which allows only for docking with either no water present or with the water present but not bound to the heme, which leads to a predicted net charge of 0 for the water. Since we docked primarily non-polar substrates, we chose to include the water molecule in the docking and accepted the incorrect charge because we deemed the steric conditions to be more important than the charges. While the choice of this software allowed us to gain access to the energetically optimized positions of substrates in the access channel and calculated affinities in these positions, it is likely that a combination of molecular dynamics studies and a different docking software that is better suited for metalloenzymes could lead to a more accurate representation of the wet-lab results.

Although not fitting with the hypothesis or docking results, the wet lab results can help gaining insight into the role of amino acids in the access channel.

Firstly, it seems that the steric properties and the space in the active site are more important to substrate preference than the chemical nature of the amino acids lining the access channel. By substituting the bulky phenylalanines with smaller, aliphatic amino acids, the enzyme variants have broader access channels, which seems to hinder alkane catalysis. The dedicated alkane monooxygenase AlkB and different varieties of P450 monooxygenase CYP153, able to hydroxylate alkanes, have access channels that are much narrower than the enzyme variants in this study, especially in the active site [23,34–36]. The three phenylalanines F69, F121 and F199 of *Aae*UPO PaDa-I, limiting the access of substrates to the heme site seem to be crucial for alkane hydroxylation (hexane and cyclohexane) of the enzyme because any alkane hydroxylation was lost with any substitution at these positions. F121 additionally seems to be the most important of the three active site phenylalanines because substitutions at these positions led to minimal or no activity for any tested substrate. Furthermore, exchanging active site phenylalanines led to surprisingly high ethylbenzene activity compared to the substitutions of phenylalanines further up in the access channel considering many dockings predicted the energetically best position to be out of reach of the heme for most variants. Possibly the substitutions in the active site do favour the correct positioning of the substrate in the access channel like discussed above (4.1.) but the effect is partially counteracted by the unfavourable distance. Lastly, the loss of cyclohexane activity for all enzyme variants is curious. While the loss of activity for substitutions close to the active site is consistent with the hexane results, even F274L, which has high ABTS and NBD activities and maintains even moderate hexane activity does not produce any cyclohexane hydroxylation products. At the moment, the authors have no explanation for how the substitution on the outer edge of the access channel (compare Fig. 1) would introduce such a substrate specific change in activity. We would like to point out that the kinetic characterisation of the variants failed. The kinetics do not correspond with any of the established kinetic models tested (e.g. Michaelis–Menten, Hill, substrate and product inhibition).

4.3. Yeast surface display as a screening tool

Furthermore, we successfully utilized yeast surface of UPOs as a screening system for enzyme variants. With this methodology it is not possible to make a distinction between expression and secretion efficiency and specific activity of the enzyme variants except by work intensive procedures described elsewhere [28]. Instead, the surface display offered the possibility to easily purify the immobilized enzymes

from the cultivation broth and concentrate them for assays by centrifugation and resuspension in enzyme storage buffer to a specific optical density. Furthermore, we were able to screen the enzyme variants in their already immobilized state. This was especially desirable because immobilization frequently reduces the activity of UPOs by substantial amounts except when using surface display as immobilization method [11,29,30,37,38]. Because this effect might be dependent on the enzyme variant, a variant that initially performed well in a free enzyme screening might lose most of its activity during immobilization. Screening yeast surface displayed variants allowed for a screening of the cumulative result of the influence of the amino acid exchange and the immobilization without adding downstream processing steps before screening, which would have reduced the amount of enzyme activity.

Although the used yeast surface display proved to be useful, it could likely be improved individually for each enzyme variant. The relatively complex genetic sequence of promoter, signal peptide, enzyme, linker and anchor protein makes it likely, that the used combination in this study, originally constructed for *Aae*UPO PaDa-I, is not optimal for every enzyme variant. An optimization for each variant could likely improve secretion and thereby activities as has been shown for different UPOs [39] without the anchor protein for surface display but would increase the amount of cloning and screening effort. Finally, we would like to mention that there may be differences in the kinetic data of the free and immobilised enzyme variants; this will be investigated in future studies.

5. Conclusion

While the *in silico* results agreed with our hypothesis, that introducing aliphatic amino acids into the access channel of *Aae*UPO PaDa-I leads to a shift in substrate preference towards aliphatic substrates, the wet-lab experiments surprisingly showed opposing results, indicating that the steric conditions in the active site are more important to the enzymes substrate specificity than the chemical nature of the amino acids. We discovered that some variants show strong differences in peroxidase/peroxygenase activity ratios compared to *Aae*UPO PaDa-I. One variant, F76L, exhibited improved ABTS and NBD activities but no variant showed an improved hexane activity, which directly contradicts the original hypothesis. Interestingly, no investigated variants catalyze the hydroxylation of cyclohexane to cyclohexanol but instead produce a different product while *Aae*UPO PaDa-I and *Hsp*UPO exclusively produce cyclohexanol (and its overoxidation product cyclohexanone) from cyclohexane.

Funding sources

Funding: This work was supported by the Deutsche Forschungsgemeinschaft [DFG, German Research Foundation, grant number 46547420]

CRediT authorship contribution statement

Niklas Teetz: Writing – original draft, Visualization, Validation, Methodology, Investigation, Formal analysis, Data curation, Conceptualization. **Sonja Schönrock:** Writing – review & editing, Visualization, Investigation. **Dirk Holtmann:** Writing – review & editing, Supervision, Resources, Project administration, Funding acquisition, Conceptualization.

Declaration of competing interest

The authors declare that they have no known competing financial interests or personal relationships that could have appeared to influence the work reported in this paper.

Acknowledgements

The authors would like to thank Selin Ertul and Lea Hoffmann for their help with wet lab work.

Supplementary materials

Supplementary material associated with this article can be found, in the online version, at doi:10.1016/j.mcat.2025.115593.

Data availability

Data will be made available on request.

References

[1] M. Hofrichter, R. Ullrich, Oxidations catalyzed by fungal peroxygenases, Curr. Opin. Chem. Biol. 19 (2014), https://doi.org/10.1016/j.cbpa.2014.01.015. /04/01.
[2] M. Hobisch, D. Holtmann, P. Gomez de Santos, M. Alcalde, F. Hollmann, S. Kara, Recent developments in the use of peroxygenases - exploring their high potential in selective oxyfunctionalisations, Biotechnol. Adv. 51 (2021) 107615, https://doi.org/10.1016/j.biotechadv.2020.107615.
[3] M. Kinne, M. Poraj-Kobielska, E. Aranda, R. Ullrich, K.E. Hammel, K. Scheibner, M. Hofrichter, Regioselective preparation of 5-hydroxypropranolol and 4′-hydroxydiclofenac with a fungal peroxygenase, Bioorg. Med. Chem. Lett. 19 (2009) 3085–3087, https://doi.org/10.1016/j.bmcl.2009.04.015.
[4] C. Aranda, R. Ullrich, J. Kiebist, K. Scheibner, J.C. del Río, M. Hofrichter, A. T. Martínez, A. Gutiérrez, Selective synthesis of the resveratrol analogue 4,4′-dihydroxy-stilbene and stilbenoids modification by fungal peroxygenases, Catal. Sci. Technol. 8 (2018) 2394–2401, https://doi.org/10.1039/c8cy00272j.
[5] S. Peter, M. Kinne, X. Wang, R. Ullrich, G. Kayser, J.T. Groves, M. Hofrichter, Selective hydroxylation of alkanes by an extracellular fungal peroxygenase, FEBS J. 278 (2011) 3667–3675, https://doi.org/10.1111/j.1742-4658.2011.08285.x.
[6] E. Churakova, M. Kluge, R. Ullrich, I. Arends, M. Hofrichter, F. Hollmann, Specific photobiocatalytic oxyfunctionalization reactions, Angew. Chem. Int. Edn. (2011) 50, https://doi.org/10.1002/anie.201105308. /11/04.
[7] T. Hilberath, R. van Oosten, J. Victoria, H. Brasselet, M. Alcalde, J.M. Woodley, F. Hollmann, Toward kilogram-scale peroxygenase-catalyzed oxyfunctionalization of cyclohexane, Org. Process. Res. Dev. 27 (2023) 1384–1389, https://doi.org/10.1021/acs.oprd.3c00135.
[8] A. Gutierrez, E.D. Babot, R. Ullrich, M. Hofrichter, A.T. Martinez, J.C. del Rio, Regioselective oxygenation of fatty acids, fatty alcohols and other aliphatic compounds by a basidiomycete heme-thiolate peroxidase, Arch. Biochem. Biophys. 514 (2011) 33–43, https://doi.org/10.1016/j.abb.2011.08.001.
[9] P.G.d. Santos, A. González-Benjumea, A. Fernandez-Garcia, C. Aranda, Y. Wu, A. But, P. Molina-Espeja, D.M. Maté, D. Gonzalez-Perez, W. Zhang, et al., Engineering a highly regioselective fungal peroxygenase for the synthesis of hydroxy fatty acids, Angew. Chem. Int. Edn. (2023) 62, https://doi.org/10.1002/anie.202217372. /02/20.
[10] Y. Ni, E. Fernandez-Fueyo, A. Gomez Baraibar, R. Ullrich, M. Hofrichter, H. Yanase, M. Alcalde, W.J. van Berkel, F. Hollmann, Peroxygenase-catalyzed oxyfunctionalization reactions promoted by the complete oxidation of methanol, Angew. Chem. Int. Ed. Engl. 55 (2016) 798–801, https://doi.org/10.1002/anie.201507881.
[11] M. Hobisch, P.d. Santis, S. Serban, A. Basso, E. Byström, S. Kara, Peroxygenase-driven ethylbenzene hydroxylation in a rotating bed reactor, Org. Process. Res. Dev. 26 (2022) 2761–2765, https://doi.org/10.1021/acs.oprd.2c00211.
[12] M. Kluge, R. Ullrich, C. Dolge, K. Scheibner, M. Hofrichter, M. Kluge, R. Ullrich, C. Dolge, K. Scheibner, M. Hofrichter, Hydroxylation of naphthalene by aromatic peroxygenase from Agrocybe aegerita proceeds via oxygen transfer from H2O2 and intermediary epoxidation, Appl. Microbiol. Biotechnol. 81 (2008), https://doi.org/10.1007/s00253-008-1704-y, 81:6 2009-01-01.
[13] A. Karich, M. Kluge, R. Ullrich, M. Hofrichter, A. Karich, M. Kluge, R. Ullrich, M. Hofrichter, Benzene oxygenation and oxidation by the peroxygenase of Agrocybe aegerita, AMB Express. 3 (2013), https://doi.org/10.1186/2191-0855-3-5, 3:1 2013-01-17.
[14] M.C. Sigmund, G.J. Poelarends, M.C. Sigmund, G.J. Poelarends, Current state and future perspectives of engineered and artificial peroxygenases for the oxyfunctionalization of organic molecules, Nat. Catal. 3 (2020), https://doi.org/10.1038/s41929-020-00507-8, 3:9 2020-09-16.
[15] M. Hofrichter, H. Kellner, R. Herzog, A. Karich, C. Liers, K. Scheibner, V.W. Kimani, R. Ullrich, Fungal peroxygenases: a phylogenetically old superfamily of heme enzym, Grand Challeng. Biol. Biotech. (2020), https://doi.org/10.1007/978-3-030-29541-7_14.
[16] M. Hofrichter, H. Kellner, R. Herzog, A. Karich, J. Kiebist, K. Scheibner, R. Ullrich, M. Hofrichter, H. Kellner, R. Herzog, et al., Peroxide-mediated oxygenation of organic compounds by fungal peroxygenases, Antioxidants 11 (2022) Page 163, https://doi.org/10.3390/antiox11010163, 2022-01-14, 11.
[17] D.T. Monterrey, A. Menés-Rubio, M. Keser, D. Gonzalez-Perez, M. Alcalde, Unspecific peroxygenases: the pot of gold at the end of the oxyfunctionalization

rainbow? Curr. Opin. Green. Sustain. Chem. 41 (2023) 100786 https://doi.org/10.1016/j.cogsc.2023.100786.
[18] C. Aranda, J. Carro, A. Gonzalez-Benjumea, E.D. Babot, A. Olmedo, D. Linde, A. T. Martinez, A. Gutierrez, Advances in enzymatic oxyfunctionalization of aliphatic compounds, Biotechnol. Adv. 51 (2021) 107703, https://doi.org/10.1016/j.biotechadv.2021.107703.
[19] E. Rytkönen, N. Hakulinen, J. Jänis, J. Rouvinen, Exploring unspecific peroxygenase selectivity with diverse hydrocarbon substrates, ChemistryOpen (2025), https://doi.org/10.1002/open.202400521.
[20] R. Ullrich, M. Poraj-Kobielska, S. Scholze, C. Halbout, M. Sandvoss, M.J. Pecyna, K. Scheibner, M. Hofrichter, Side chain removal from corticosteroids by unspecific peroxygenase, J. Inorg. Biochem. 183 (2018), https://doi.org/10.1016/j.jinorgbio.2018.03.011. /06/01.
[21] E. Aranda, R. Ullrich, M. Hofrichter, E. Aranda, R. Ullrich, M. Hofrichter, Conversion of polycyclic aromatic hydrocarbons, methyl naphthalenes and dibenzofuran by two fungal peroxygenases, Biodegradation 21 (2009), https://doi.org/10.1007/s10532-009-9299-2, 21:2 2009-09-22.
[22] A. Karich, R. Ullrich, K. Scheibner, M. Hofrichter, Fungal unspecific peroxygenases oxidize the majority of organic EPA priority pollutants, Front. Microbiol. 8 (2017), https://doi.org/10.3389/fmicb.2017.01463.
[23] X. Guo, J. Zhang, L. Han, J. Lee, S.C. Williams, A. Forsberg, Y. Xu, R.N. Austin, L. Feng, Structure and mechanism of the alkane-oxidizing enzyme AlkB, Nat. Commun. 14 (2023) 2180, https://doi.org/10.1038/s41467-023-37869-z.
[24] P. Molina-Espeja, E. Garcia-Ruiz, D. Gonzalez-Perez, R. Ullrich, M. Hofrichter, M. Alcalde, Directed evolution of unspecific peroxygenase from Agrocybe aegerita, Appl. Environ. Microbiol. 80 (2014) 3496–3507, https://doi.org/10.1128/aem.00490-14.
[25] F. Schmitz, M. Hoffrogge, K. Koschorreck, Y. Fukuta, A. Raffaele, F. Tieves, T. Hilberath, F. Hollmann, V.B. Urlacher, Identification of key active-site positions controlling the chemoselectivity of Aspergillus Brasiliensis unspecific peroxygenase, Chembiochem. 26 (2025), https://doi.org/10.1002/cbic.202500181. /05/27.
[26] A. Knorrscheidt, J. Soler, N. Hünecke, P. Püllmann, M. Garcia-Borràs, M. J. Weissenborn, Accessing chemo- and regioselective benzylic and aromatic oxidations by protein engineering of an unspecific peroxygenase, ACS Catal. (June 7, 2021) 11, https://doi.org/10.1021/acscatal.1c00847.
[27] L. Rotilio, A. Swoboda, K. Ebner, C. Rinnofner, A. Glieder, W. Kroutil, A. Mattevi, Structural and biochemical studies enlighten the unspecific peroxygenase from hypoxylon sp. EC38 as an efficient oxidative biocatalyst, ACS Catal. (September 2, 2021) 11, https://doi.org/10.1021/acscatal.1c03065.
[28] N. Teetz, S. Lang, A. Liese, D. Holtmann, Yeast surface display enables one-step production and immobilization of unspecific peroxygenases, ChemCatChem (2024), https://doi.org/10.1002/cctc.202400908.
[29] N. Teetz, A.L. Drommershausen, L. Gebele, D. Holtmann, Holistic evaluation of enzyme immobilization processes: a method for evaluating the entire production process, ChemCatChem (2025), https://doi.org/10.1002/cctc.202500699.
[30] P.d. Santis, N. Petrovai, L.E. Meyer, M. Hobisch, S. Kara, A holistic carrier-bound immobilization approach for unspecific peroxygenase, Front. Chem. 10 (2022) 985997, https://doi.org/10.3389/fchem.2022.985997.
[31] A. Olmedo, C. Aranda, J.C.d. Río, J. Kiebist, K. Scheibner, A.T. Martínez, A. Gutiérrez, From Alkanes to carboxylic acids: terminal oxygenation by a fungal peroxygenase, Angew. Chem. Int. Edn. (2016) 55, https://doi.org/10.1002/anie.201605430. /09/26.
[32] D. Linde, E. Santillana, E. Fernández-Fueyo, A. González-Benjumea, J. Carro, A. Gutiérrez, A.T. Martínez, A. Romero, D. Linde, E. Santillana, et al., Structural characterization of two short unspecific peroxygenases: two different dimeric arrangements, Antioxidants 11 (2022), https://doi.org/10.3390/antiox11050891. Page 891 2022-04-30, 11.
[33] N. Teetz, L. Zuhse, D. Holtmann, N. Teetz, L. Zuhse, D. Holtmann, Optimizing yeast surface-displayed unspecific peroxygenase production for sustainable biocatalysis, Bioengineering 12 (2025), https://doi.org/10.3390/bioengineering12080822. Vol. 12, Page 822 2025-07-30.
[34] E.G. Funhoff, U. Bauer, I.s. García-Rubio, B. Witholt, J.B.v. Beilen, CYP153A6, a soluble P450 oxygenase catalyzing terminal-alkane hydroxylation, J. Bacteriol. (2006), https://doi.org/10.1128/jb.00286-06. -July-15.
[35] D.J. Koch, M.M. Chen, J.B.v. Beilen, F.H. Arnold, In vivo evolution of butane oxidation by terminal alkane hydroxylases AlkB and CYP153A6, Appl. Environ. Microbiol. 75 (2009), https://doi.org/10.1128/AEM.01758-08. -January-15.
[36] C.L. Jacobs, R.d. Aido-Machado, C. Tolmie, M.S. Smit, D.J. Opperman, C.L. Jacobs, R. do Aido-Machado, C. Tolmie, M.S. Smit, D.J. Opperman, CYP153A71 from Alcanivorax dieselolei: oxidation beyond monoterminal hydroxylation of n-alkanes, Catalysts 12 (2022), https://doi.org/10.3390/catal12101213. Vol. 12, Page 1213 2022-10-11.
[37] S. Bormann, B.O. Burek, R. Ulber, D. Holtmann, Immobilization of unspecific peroxygenase expressed in Pichia pastoris by metal affinity binding, Mol. Catal. 492 (2020) 110999, https://doi.org/10.1016/j.mcat.2020.110999.
[38] P. Molina-Espeja, P. Santos-Moriano, E. García-Ruiz, A. Ballesteros, F.J. Plou, M. Alcalde, Structure-guided immobilization of an evolved unspecific peroxygenase, Int. J. Mol. Sci. (2019) 20, https://doi.org/10.3390/ijms20071627.
[39] P. Püllmann, M.J. Weissenborn, Improving the heterologous production of fungal peroxygenases through an episomal pichia pastoris promoter and signal peptide shuffling system, ACS Synth. Biol. (June 2, 2021) 10, https://doi.org/10.1021/acssynbio.0c00641.